

Influence of Power Frequency Magnetic Field Interference in Substation on 5G Base Station Deployment

Hai Chuan Niu, Jie-Qing Fan^{*}, and Tian Hao Hou

Abstract—The limited space of the substation contains a lot of electrical equipment and voltages ranging from hundreds to several thousand volts, resulting in a complex electromagnetic environment in the substation. As the deployment of 5G base stations increases in substations in China, the power-frequency magnetic field in substations will cause problems, resulting in a location problem. This paper develops a circuit model for converter stations and presents a calculation method that considers the geomagnetic permeability, 3-phase transmission mode, and erection direction influences. The correctness of the calculation method in this paper is verified by comparing the simulation results and calculation results of the substation model. The deployment conditions of 5G base stations in the substation are analyzed according to the national standard of the requirement and measurement methods of electromagnetic compatibility for mobile telecommunications equipment Part 17: 5G base station and ancillary equipment.

1. INTRODUCTION

As key technical support for smart grid construction, 5G communication base stations have been gradually deployed in power grid transmission and substation systems in recent years [1]. Substations possess an array of electrical equipment voltage levels to vary from dozens to thousands of kV, including arresters, circuit breakers, isolation switches, and secondary equipment for control and protection, resulting in a complex electromagnetic environment [2]. Electric field interference and magnetic field interference greater than 100 Hz can be shielded usually by 5G equipment deployed in substations with metal shielding shells, but power frequency magnetic field interference (50 Hz) can hardly be shielded [3]. Additional factors affecting the safety distance of a 5G station include line voltage levels, magnetic field interference, and power frequency differences in a substation. The construction of the 5G communication network has contributed to China's technological advancement in smart grid technology. However, the electromagnetic compatibility research of 5G base station equipment in the substation is still in its infancy, and there is a lack of national standard documents.

Researchers currently focus on the following aspects of power frequency magnetic field in substations: (1) Magnetic field distribution of typical large electrical equipment in the substation, such as magnetic field intensity of air-core reactor in large substation [3]. (2) In substations, magnetic field distributions are studied by the finite element or moment method, with research primarily focused on the typical electrical equipment in the substation [4, 5]. (3) Substation electrical equipment, control, and protection equipment are affected by high-frequency electromagnetic waves generated by surge impacts and switch transient changes. Magnetic field calculation in a substation is complex, and the magnetic field calculation theory cannot be applied simply. In addition to the incoming and outgoing lines and the large electrical equipment, the influencing factors should also be considered according to the actual situation in the substation [6]. Ref. [7, 8] use the finite element method to calculate the

Received 3 August 2022, Accepted 7 September 2022, Scheduled 26 September 2022

^{*} Corresponding author: Jie-Qing Fan (fanjieqing@ncepu.edu.cn).

The authors are with the College of Electrical and Electronic Engineering, North China Electrical Power University, Beijing, China.

substation frequency magnetic field distribution, which greatly increases the calculation difficulty and limits the range of the calculation. Refs. [9–11] use different numerical methods to calculate magnetic fields and consider only the distribution of magnetic fields in the substation area, without considering the influencing factors. The purpose of this paper is to explore a calculation method that considers the influence factors of the power frequency magnetic field within the substation and analyzes the deployment conditions of 5G communication equipment within it.

Based on Biot-Savart law, this paper selects a real-world substation as the subject of the research, establishes a model for the line, and proposes a method of calculating the frequency magnetic field inside the substation. The accuracy of the proposed method is verified by comparing the theoretical calculation method with FEKO (3D full-wave electromagnetic simulation software) simulation calculation results, and in order to give deployment recommendations for 5G base station equipment the calculation results are compared with national standards to obtain the deployment.

2. CALCULATION OF POWER FREQUENCY MAGNETIC FIELD IN SUBSTATION

High voltage levels in the substation produce a strong magnetic field interference, and metal shielding shells of 5G equipment have almost no effect on it; therefore, it will be the main cause of problems for 5G equipment and secondary equipment. As shown in Figure 1, a calculation model of the power frequency magnetic field in the substation is used to estimate the influence that the field has on 5G communication equipment.

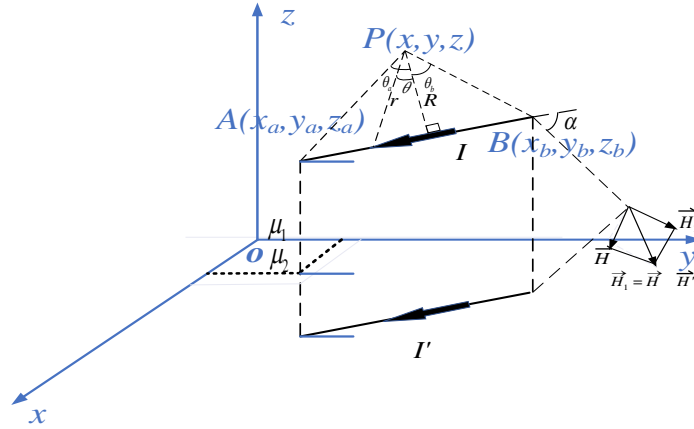


Figure 1. Calculation model of substation frequency magnetic field.

In the substation, transmission line sag and long-distance transmission span are not considered since the distance of the transmission line is short. Following are the assumptions made before examining and calculating the influence of geomagnetic permeability: 1. The earth is treated as an infinite magnetic medium. 2. The transmission line is located above the earth, and the direction is arbitrary, with the transmission line from the ground height h . 3. The magnetic permeabilities of the two sides of the interface are μ_1 (air magnetic permeability) and μ_2 (earth magnetic permeability).

According to the calculation model diagram shown in Figure 1, the current element vector at a point in space is decomposed into the sum of the three components of the coordinate axes, shown as follows.

$$IdI = Idxe_x + Idxe_y + Idxe_z \quad (1)$$

In formula (1), e_x , e_y , e_z is the magnetic-field vector in x , y , z direction.

According to [11], the uniqueness of the magnetic field solution can be determined if the current element in the effective region remains unchanged. Therefore, the expressions of the current in any direction and the mirror current in the space are shown as follows.

$$I' = \frac{\mu_2 - \mu_1}{\mu_2 + \mu_1} I \quad (2)$$

For the electrified wire with length l_{ab} in space, according to the Biot-Savart law and the mirror current derived above, the magnetic field generated by the current element at any point in the space is shown in Formula (3).

$$d\vec{B} = \frac{\mu_0}{4\pi} \frac{I d\vec{l} \times \vec{r}}{r^3} = \frac{\mu_0}{4\pi} \frac{I dl \sin \theta}{r^2} \vec{e}_B \quad (3)$$

In Formula (3), I is the current intensity, $d\vec{l}$ the line element of the source current, μ_0 the vacuum permeability, \vec{r} the position vector of the current element to point p , e_B the magnetic field direction of point in space, and θ the angle between the current element and \vec{r} . The magnetic field expression generated by the point of the current element in the space in Formula (2) is integrated, and the mirror current mentioned above is brought in. The magnetic field intensity can be expressed as follows:

$$\vec{B} = \frac{\mu_0}{4\pi\rho} (\sin \theta_a + \sin \theta_b) \left(I + \frac{\mu_2 - \mu_1}{\mu_2 + \mu_1} I \right) \vec{e}_B \quad (4)$$

By using Equation (4), we can determine the magnetic field intensity generated by the straight wire at a point p in space. For the calculation of the magnetic field of any angle transmission line in the substation, first of all, the calculation model of the coordinate system $o-xyz$ translation changes to the origin of the current-carrying wire A point, $P(x, y, z)$ after coordinate transformation for $P'(xx, yy, zz)$, and then rotate the coordinate system to AB extended $o'-x'$ direction and overlap, $P'(xx, yy, zz)$ after coordinate transformation for $P''(x', y', z')$. The coordinate translation and rotation transformation model diagram is shown in Figure 2.

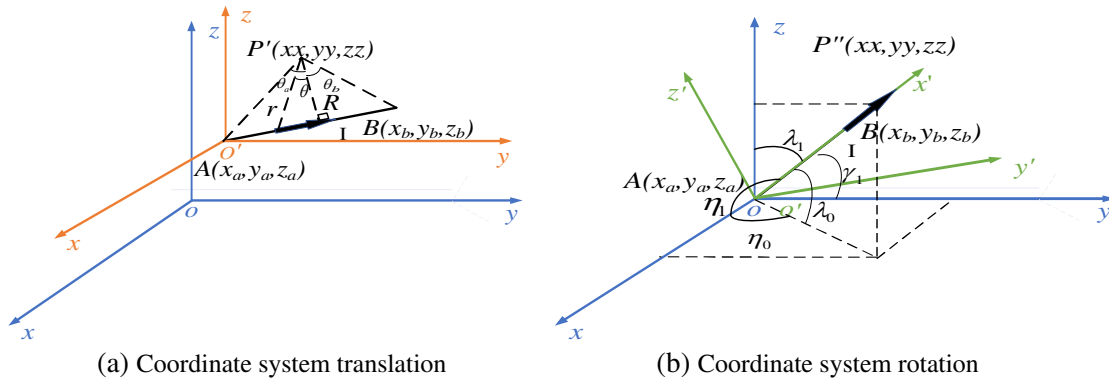


Figure 2. Coordinate transformation model diagram: (a) Coordinate system translation; (b) Coordinate system rotation.

After coordinate transformation, matrix transformation theory predicts the following expression (5):

$$\begin{bmatrix} x' \\ y' \\ z' \end{bmatrix} = \begin{bmatrix} \cos \eta_1 & \cos \eta_2 & \cos \eta_3 \\ \cos \gamma_1 & \cos \gamma_2 & \cos \gamma_3 \\ \cos \lambda_1 & \cos \lambda_2 & \cos \lambda_3 \end{bmatrix}^{-1} \begin{bmatrix} x - x_1 \\ y - y_1 \\ z - z_1 \end{bmatrix} \quad (5)$$

In Formulas (2)–(5), $\eta_1, \gamma_1, \lambda_1$ are the orientation angles of the new coordinate system ‘ $O'x'$ ’ in $o'-xyz$; $\eta_2, \gamma_2, \lambda_2$ are the orientation angles of $o'y'$ in the coordinate system $o'-xyz$; $\eta_3, \gamma_3, \lambda_3$ are the orientation angles of ‘ Oz' ’ in the coordinate system $O'-xyz$. Transformation of magnetic field between (B_X, B_Y, B_Z) and (B'_X, B'_Y, B'_Z) can be expressed as:

$$\begin{bmatrix} B_x \\ B_y \\ B_z \end{bmatrix} = \begin{bmatrix} \cos \eta_1 & \cos \eta_2 & \cos \eta_3 \\ \cos \gamma_1 & \cos \gamma_2 & \cos \gamma_3 \\ \cos \lambda_1 & \cos \lambda_2 & \cos \lambda_3 \end{bmatrix} \begin{bmatrix} B'_x \\ B'_y \\ B'_z \end{bmatrix} \quad (6)$$

According to [12], when the current-carrying straight wire l_{ab} coincides with the x -axis in the space, the current direction is the positive direction of x -axis, and the magnetic field expression of any point

p in the space is:

$$\begin{cases} B_x = 0 \\ B_y = \left(I + \frac{\mu_2 - \mu_1}{\mu_2 + \mu_1} \right) \frac{\mu_0 z}{4\pi(x^2 + y^2)} \cdot \frac{x - L}{\sqrt{(x - L)^2 + y^2 + z^2}} \cdot \frac{x}{\sqrt{x^2 + y^2 + z^2}} \\ B_z = \left(I + \frac{\mu_2 - \mu_1}{\mu_2 + \mu_1} \right) \frac{\mu_0 y}{4\pi(y^2 + z^2)} \cdot \frac{x}{\sqrt{x^2 + y^2 + z^2}} \cdot \frac{x - L}{\sqrt{(x - L)^2 + y^2 + z^2}} \end{cases} \quad (7)$$

Therefore, when calculating the power frequency magnetic field intensity in the spatial range of several transmission lines and transmission lines erected at any angle, it is only necessary to know the coordinates of each break point in the transmission line and the magnetic field component of the straight line segment. After superposition, the power frequency magnetic field intensity can be obtained.

Most of the transmission modes in substations adopt three-phase AC transmission modes with the same frequency, the same potential amplitude, and 120° phase difference. Therefore, when calculating the magnetic field strength of the three-phase current-carrying conductors in space, it is necessary to set the phase angle for the current-carrying conductors in the transmission line τ ($\tau_A = 0^\circ$, $\tau_B = -120^\circ$, $\tau_C = 120^\circ$). According to the superposition theorem, the total magnetic field intensity of point P can be obtained by superimposing the magnetic field intensity B_{xN} , B_{yN} , B_{zN} generated by the ABC three-phase transmission conductor extending along x , y , and z directions. Therefore, the total magnetic field strength at P point can be expressed as:

$$B = \sqrt{B_{xN}^2 + B_{yN}^2 + B_{zN}^2} \quad (8)$$

3. ALGORITHM VALIDATION

Taking the transmission line of a substation as the model, the substation is divided into 500 kV and 220 kV areas to verify the correctness of the calculation method of the power frequency magnetic field of the substation. The layout diagram and overall model diagram of the substation are shown in Figure 3.

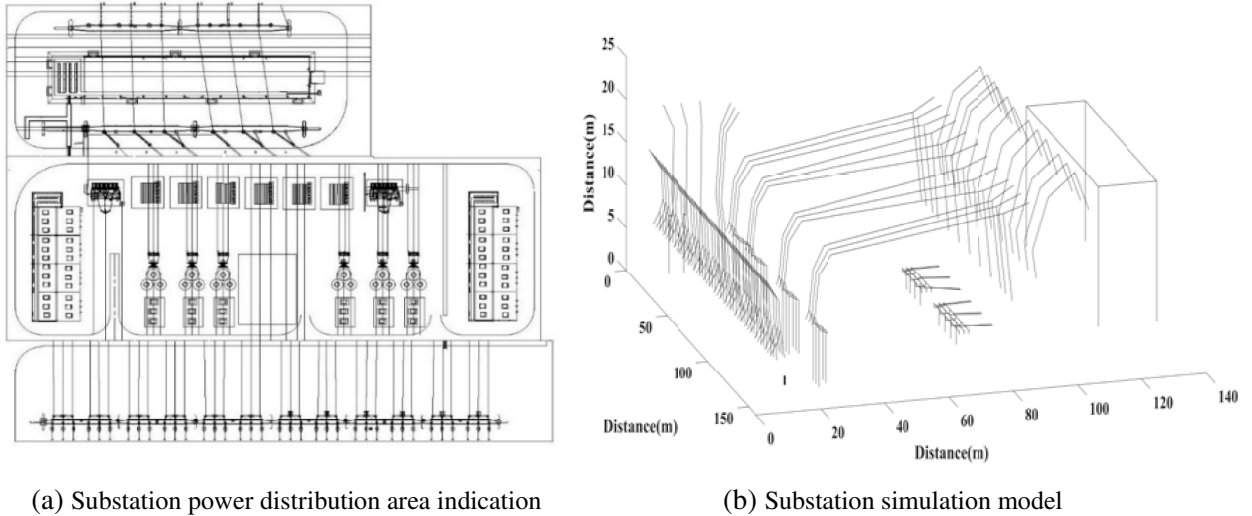


Figure 3. Simulation Model of Actual station: (a) Substation power distribution area indication; (b) Substation simulation model.

Because of the large amount of electrical equipment in the substation, transmission lines are numerous and irregular, and the size of the power frequency magnetic field in the substation is mainly related to the current in the current carrying conductor, so the simplified treatment of the bus and the wire between the pieces of equipment in the substation is carried out. Do not consider the substation circuit breaker, disconnector, and other electrical equipment.

The ground material for substation construction depends on the construction environment and design requirements of the substation, and is usually concrete or brick. It is common for various kinds of cracks to appear after a period of time of substation operation, such as cracking, shrinkage cracks, and surface cracks formed by the bottom cracking, resulting in errors in calculations. Solar storms with periods of 8–14 years will cause geomagnetic disturbances (GMD), which will affect electrical equipment such as transformers [13]. In order to calculate power frequency magnetic fields closely related to substation operation, transmission lines erected arbitrarily with a certain angle should be taken into account. It is thus recommended to use the geomagnetic permeability and transmission lines erected arbitrarily as the variable when verifying the accuracy of the calculation results of the power frequency magnetic field in the substation.

According to the factors affecting the power frequency magnetic field in the substation mentioned above, the earth permeability in the substation and the transmission line angle in the substation are changed. The calculation methods and simulation models derived above are used to compare and verify the following examples.

Calculation example 1: Earth’s magnetic permeability is $3.74\pi \times 10^{-7} \text{ N/A}^2$. The current amplitude of the transmission line is 1200 A, and the phase is $0^\circ, 180^\circ, 120^\circ, 300^\circ, 60^\circ, -120^\circ$.

Calculation example 2: Earth’s magnetic permeability is $12.83\pi \times 10^{-7} \text{ N/A}^2$. The current amplitude of the transmission line is 1200 A, and the phase is $0^\circ, 180^\circ, 120^\circ, 300^\circ, 60^\circ, -120^\circ$.

Calculation example 3: The substation model contains 500 kV, 220 kV voltage levels, with transmission lines parallel to the ground. The current amplitude of the transmission line is 1200 A, and the phase is $0^\circ, 180^\circ, 120^\circ, 300^\circ, 60^\circ, -120^\circ$. Magnetic field calculation example.

Calculation example 4: Substation model contains 500 kV, 220 kV voltage levels, and transmission lines are erected arbitrarily. The current amplitude of the transmission line is 1200 A, and the phase is $0^\circ, 180^\circ, 120^\circ, 300^\circ, 60^\circ, -120^\circ$. Magnetic field calculation example.

The actual transmission line model of the actual substation is established to change the geomagnetic permeability. The power frequency magnetic field calculation theory and software simulation results are compared and verified. The calculation results are shown in Figure 4.

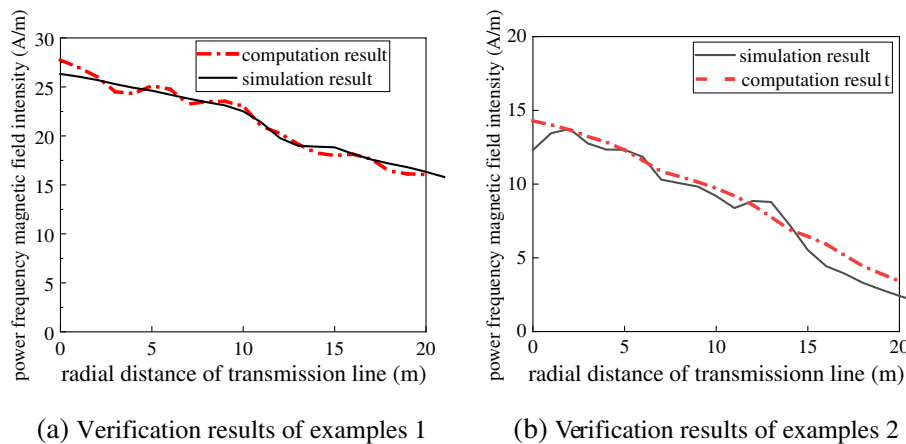


Figure 4. Verification results of power frequency magnetic field of examples 1 and 2.

According to Figure 4, it can be seen that with changing the geomagnetic permeability, the calculated and simulated results have the same trend. In example 1, when the radial distance of transmission line is 0 m, the computation and simulation result of power frequency magnetic field intensity is maximum, and the value is about 26 A/m, when the radial distance of transmission line is 20 m, the computation and simulation result of power frequency magnetic field intensity is minimum, and the value is about 15 A/m. Using the average error calculation method, it can be concluded that the error between the calculation and simulation results in example 1 is less than 5.7%. In example 2, when the radial distance of transmission line is 0 m, the computation and simulation result of power frequency magnetic field intensity is maximum, and the value is about 13 A/m. When the radial distance

of transmission line is 20 m, the computation and simulation result of power frequency magnetic field intensity is minimum, and the value is about 3 A/m. Using the average error calculation method, it can be concluded that the error between the calculation results and simulation results in example 2 is less than 6.4%, indicating the accuracy and effectiveness of the calculation method. Because of the different ground materials and thicknesses of the actual substation, the geomagnetic permeability also changes. In the consumable land, due to the displacement of the current, the resistance increases with the increase of the frequency, and the inductance decreases with the increase of the frequency. With the increase of the permeability of the earth, the geomagnetic flux increases, and the resistance and inductance increase, which affects the calculation results of the power frequency magnetic field in the substation.

Figure 5 shows the frequency magnetic field intensity distribution in the substation with different geodesic permeabilities according to the substation parameters of calculation example 1 and calculation example 2, respectively.

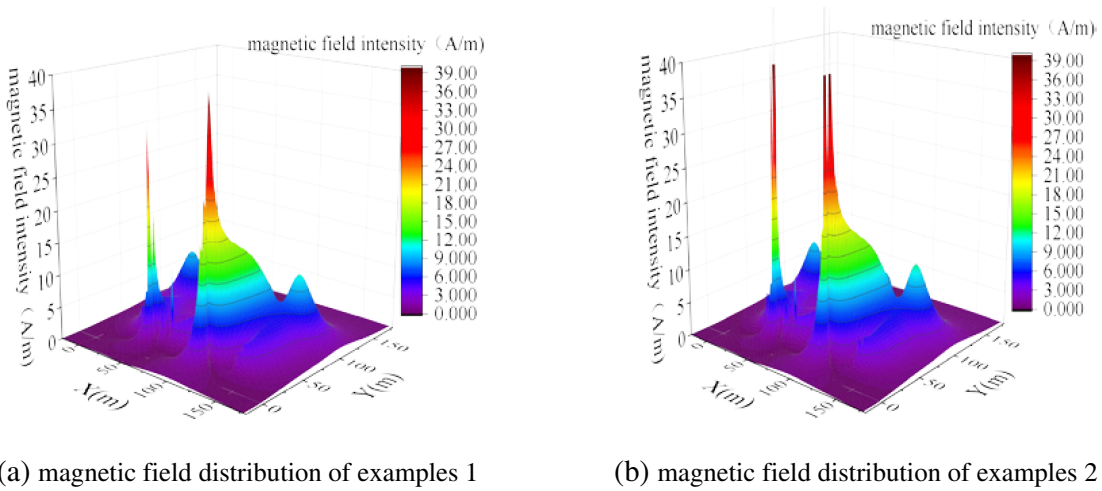


Figure 5. Distribution results of power frequency magnetic field in examples 1 and 2.

Taking a substation as an example, a simulation model of parallel and arbitrary angle distribution of substation transmission lines is established. The theoretical calculation method and simulation results of the power frequency magnetic field in the substation are compared and verified, and the calculation results are shown in Figure 6.

According to Figure 6, it can be seen that in different transmission line erection directions, the calculated results and simulation results have the same trend, and the error is small. In example 3,

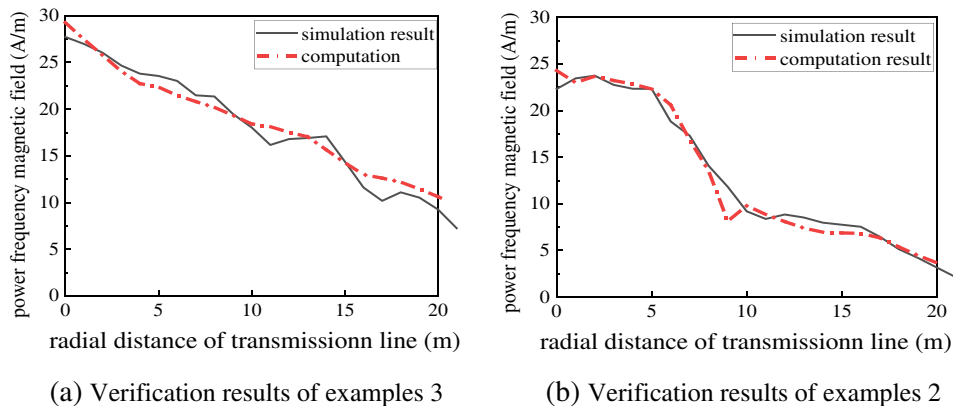
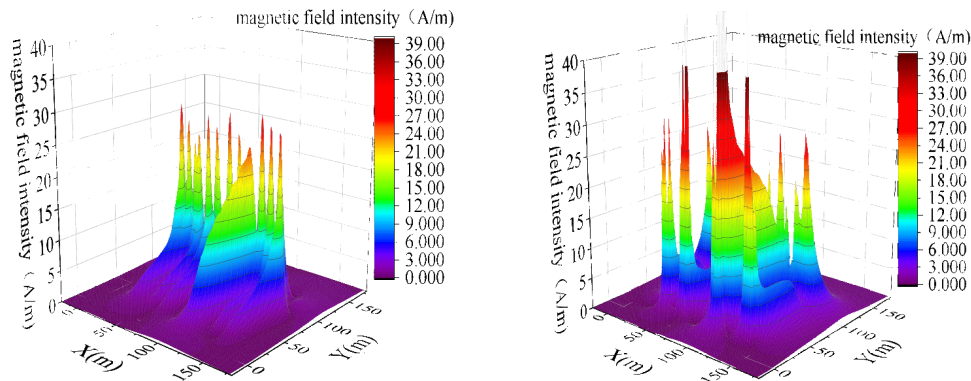


Figure 6. Verification results of power frequency magnetic field of examples 3 and 4.

when the radial distance of transmission line is 0 m, the computation and simulation result of power frequency magnetic field intensity is maximum, and the value is about 28 A/m. When the radial distance of transmission line is 20 m, the computation and simulation result of power frequency magnetic field intensity is minimum, and the value is about 8 A/m. Using the average error calculation method, it can be concluded that the error between the calculation results and simulation results in example 3 is less than 4.9%. In example 4, when the radial distance of transmission line is 0 m, the computation and simulation result of power frequency magnetic field intensity is maximum, and the value is about 23 A/m. When the radial distance of transmission line is 20 m, the computation and simulation result of power frequency magnetic field intensity is minimum, and the value is about 2 A/m. Using the average error calculation method, it can be concluded that the error between the calculation results and simulation results in example 4 is less than 5.2% indicating the accuracy and effectiveness of the calculation method. Figures 6 shows the substation frequency magnetic field intensity distribution for transmission lines erected parallel to the ground and erected at any angle according to the substation parameters of example 3 and example 4, respectively.

According to Figure 4 to Figure 7, it can be seen that the calculation results using the calculation method proposed in this paper and the simulation of the substation's frequency magnetic field are almost the same, and the error does not exceed 7%. It proves the effectiveness of this paper's calculation method of the frequency magnetic field in substations considering the geodesic permeability and three-phase transmission lines. The calculation method in this paper can not only calculate the spatial magnetic field with complex electrical structures in substations but also be used to calculate the spatial transient power frequency magnetic field generated by simple high voltage transmission lines.



(a) magnetic field distribution of examples 3 (b) magnetic field distribution of examples 1

Figure 7. Distribution results of power frequency magnetic field in examples 3(a) and 4(b).

4. IMPACT OF INDUSTRIAL FREQUENCY MAGNETIC FIELDS IN SUBSTATIONS ON THE DEPLOYMENT OF 5G BASE STATIONS

Consider that 5G devices are placed outside the substation. The antenna erection height in China is usually within the range of 2 m–50 m on the ground. Therefore, to analyze the distribution of the power frequency magnetic field at different heights in the substation, the power frequency magnetic field strength of the substation 1 m–55 m away from the ground is calculated in the simulation calculation.

By comprehensively comparing the Electromagnetic compatibility — Generic standards — Immunity for power station and substation environments (GBZ 17799.6-2017) and Requirement and measurement methods of electromagnetic compatibility for mobile telecommunications equipment Part 17: 5G base station and ancillary equipment (YD/T 2583.17-2019), it is found that the standard limits of power frequency magnetic field in the two national standard documents are set to 3 A/m, so the power frequency magnetic field limit of 5G communication equipment in substations is set to 3 A/m.

Based on the calculation method of substation power frequency magnetic field show in Equations (1)–(8), according to the comparison of the two national standards mentioned above, the

power frequency magnetic field limit is set to 3 A/m. The overhead line height and line current intensity settings in Table 1 are based on the actual operation of the substation corresponding voltage level transmission line parameters; therefore, the accurate deployment range of 5G communication equipment under different heights of transmission lines with different voltage levels in the substation can be obtained, as shown in Table 1.

Table 1. 5G equipment deployment security range at different heights (frequency magnetic field less than 3 A/m).

height	Safe distance of 5G equipment deployed around 110 kv overhead conductor	Safe distance of 5G equipment deployed around 220 kv overhead conductor	Safe distance of 5G equipment deployed around 500 kv overhead conductor
	(Overhead line height approximately 7 m) Line current about 270 A Limit 3 A/m	(Overhead line height approximately 18 m) Line current about 400 A Limit 3 A/m	(Overhead line height approximately 22 m) Line current about 1200 A Limit 3 A/m
1 m	10.3 m	12.3 m	21.4 m
2 m	10.5 m	13.6 m	22.3 m
4 m	12.1 m	14.4 m	22.8 m
6 m	13.7 m	15.3 m	24.3 m
8 m	13.4 m	16.7 m	25.1 m
10 m	11.4 m	17.5 m	26.7 m
12 m	10.7 m	18.1 m	27.4 m
14 m	8.6 m	18.8 m	28.3 m
16 m	6.8 m	20.1 m	29.2 m
18 m	6.2 m	21.4 m	29.9 m
20 m	4.4 m	20.8 m	31.5 m
22 m	3.5 m	19.9 m	32.7 m
24 m	2.7 m	18.7 m	31.8 m
26 m	conformation of standard	17.1 m	28.4 m
28 m	conformation of standard	15.6 m	23.7 m
30 m	conformation of standard	13.8 m	21.5 m
32 m	conformation of standard	10.1 m	18.9 m
34 m	conformation of standard	8.4 m	14.4 m
36 m	conformation of standard	6.2 m	11.9 m
38 m	conformation of standard	3.3 m	8.6 m
40 m	conformation of standard	conformation of standard	5.7 m
42 m	conformation of standard	conformation of standard	3.3 m
44 m	conformation of standard	conformation of standard	2.1 m
46 m	conformation of standard	conformation of standard	conformation of standard
48 m	conformation of standard	conformation of standard	conformation of standard
50 m	conformation of standard	conformation of standard	conformation of standard

According to the data in Table 1, it can be seen that in the same voltage level, with the increase of height, the security range of 5G communication equipment deployment also increases and reaches the maximum when the height increases to the height of the overhead line. After exceeding the height of the overhead line, the security range gradually decreases to 0.

The power frequency magnetic field distribution of substations with different voltage levels at typical heights is shown in Figure 8.

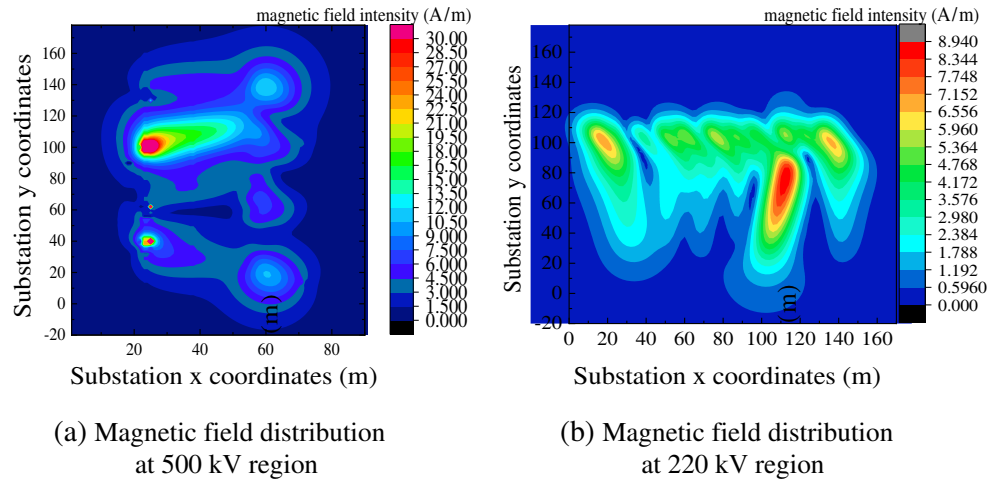


Figure 8. Distribution results of power frequency magnetic field in 500 kV region (a) and 220 kV region (b).

After a comprehensive analysis of the results of the frequency magnetic field distribution at different heights of 500 kV and 220 kV transmission lines in the substation, we can get the recommendation of 5G base station deployment in the substation: 1) the magnetic field strength of the 500 kV line may exceed 3 A/m within a radius of about 32.7 m around the ground projection position, so 5G equipment cannot be deployed in the area; 2) the magnetic field strength of the 220 kV line may exceed 3 A/m within a radius about 21.4 m around the ground projection, so 5G equipment cannot be deployed in the area.

5. CONCLUSIONS

This paper uses the combination of the superposition method and mirror current method to calculate the calculation method of the substation's industrial frequency magnetic field considering the geodesic permeability, three-phase transmission mode, and transmission line erection direction, respectively, which can calculate the industrial frequency magnetic field in substations with different voltage levels of transmission lines and larger space, avoiding the limit value problem when using the finite element method for magnetic field calculation. The accuracy of power frequency magnetic field calculation is verified by simulation modeling and theoretical calculation, which can be used as a theoretical basis for the deployment of 5G base stations in substations. Finally, the deployment conditions of 5G communication equipment in the substation are obtained by combining the calculation results of the power frequency magnetic field in the substation with the national standard of 5G communication equipment immunity.

REFERENCES

1. Huang, Y., H. Yu, J. Yin, G. Meng, and Y. Cheng, "Power IoT data transmission scheme: Current status and outlook based on 5G technology," *Journal of Electrical Engineering Technology*, Vol. 36, No. 17, 3581–3593, 2021, DOI: 10.19595/j.cnki.1000-6753.tces.201464.

2. Wang, Z., Y. Hu, S. Meng, H. Zhang, L. Teng, and S. Zhu, "Research on location selection method of 5G base station in substation considering radiation disturbance and conduction disturbance," *2022 International Conference on Computer Communication and Informatics (ICCCI)*, 1–8, 2022, DOI: 10.1109/ICCCI54379.2022.9741047.
3. Qin, Y. and S. A. Sebo, "Accurate evaluation of the magnetic field strength of large substation air-core reactor coils," *IEEE Transactions on Power Delivery*, Vol. 13, No. 4, 1114–1119, 2002.
4. Kangozhin, B. R., M. S. Zharmagambetova, S. S. Dautov, et al., "Electromagnetic compatibility of high voltage substation SMART devices," *Physical Sciences and Technology*, Vol. 7, Nos. 1–2, 48–55, 2020.
5. Hasselgren, L. and E. Moller, "Calculation of magnetic shielding of a substation at power frequency using FEM," *IEEE Transactions on Power Delivery*, Vol. 9, No. 3, 1398–1405, 1994.
6. Xin, C., "Research and analysis of transient electromagnetic interference in substation switching operation," *Electrical Engineering*, 2016.
7. Wang, Q., Y. Zhang, Y. Li, et al., "Frequency magnetic field distribution around a dry hollow reactor," *Journal of Electrical Engineering Technology*, Vol. 24, No. 1, 8–13, 2009.
8. Li, Y. M., L. W. Xu, J. H. Yu, et al., "35kV dry hollow reactor under frequency magnetic field suppression," *High Voltage Technology*, Vol. 36, No. 12, 2960–2965, 2010.
9. Bai, F., L. Qi, X. Cui, et al., "Prediction of steady-state electromagnetic disturbance characteristics of ultra-high voltage substations," *High Voltage Technology*, Vol. 35, No. 8, 1836–1840, 2009.
10. Du, Z., J. Ruan, C. Gan, et al., "Three-dimensional numerical simulation study of frequency electromagnetic field in substation," *Power Grid Technology*, Vol. 36, No. 4, 229–235, 2012.
11. Xin, L., "Study of 220kV substation industrial frequency magnetic field," *Electrical Engineering Technology*, Vol. 11, No. 15, 14–16, 2007.
12. Wang, Z.-Z., B.-X. Lu, and B.-G. Wang, "Three-dimensional representation of constant magnetic field mirror method," *Proceedings of the Second National Seminar on Teaching Reform of Electrical Engineering and Its Automation in Colleges and Universities (Next Volume)*, 72–77, 2004.
13. Halbedl, T. S., H. Renner OVE, and G. Achleitner OVE, "Analysis of the impact of geomagnetic disturbances on the Austrian transmission grid," *Elektrotechnik und Informationstechnik*, Vol. 134, No. 1, 67–70, 2017.